RESEARCH ARTICLE

The most comprehensive history of fire activity in the Pur-Taz interfluve over the last 11,000 years (Western Siberia, Russia)

Nikita V. Shefer[1], Sergey V. Loiko[1], Ivan V. Krickov[1], Artem G. Lim[1]

1 *Tomsk State University, 36 Lenin Ave., Tomsk, 634050, Russia*

Corresponding author: Nikita V. Shefer (vchifz@mail.ru)

Citation: Shefer NV, Loiko SV, Krickov IV, Lim AG (2024) The most comprehensive history of fire activity in the Pur-Taz interfluve over the last 11,000 years (Western Siberia, Russia). Acta Biologica Sibirica 10: 1755–1777. https://doi.org/10.5281/zenodo.14525710

Abstract

Climate change in the Arctic may increase the incidence of tundra fires, which is expected to significantly transform tundra ecosystems. Therefore, it is promising to study the tundra paleofire data to assess whether the projected increase in fire numbers is unique. In this study, we used five types of ancient fire proxies to estimate the number of fire events during the Holocene in the southern tundra of Western Siberia. Our integrated analysis of soil and peat deposit proxies allowed us to distinguish, for the first time, three different fire activity periods for this region. In the first period from 11.2 to 7.5 cal kyr BP, high fire activity was recorded. In the second period from 7.5 to 3.5 cal kyr BP the number of fire events is minimal. In the third period from 3.5 cal kyr BP to the present day, the number of pyrogenic events is maximum, and the maximum occurs in the second and third millennia from our days. For the third period, a temporal relationship between fire frequency and archaeological cultures is noted. It was also established that in the second half of the Holocene in the southern tundra peat accumulation was not interrupted in fens permafrost polygonal peat plateaus. This allowed us to obtain a good time resolution of the peat charcoal record for the last 3.5 thousand years. Thus, this study demonstrates the occurrence of landscape fires in the southern tundra throughout the Holocene. And the predicted increase in the frequency of tundra fires has paleoecological analogues.

Keywords

Paleofire, macro-charcoal, micro-charcoal, non-pollen palynomorphs (NPP), soil charcoal, Yamalo-Gydan ecoregion

Introduction

Landscape fires are an ancient and widespread exogenous ecological factor causing significant changes in biocenoses, altering the ratio of individual groups of living organisms (Kelly et al. 2020; Certini et al. 2021). The impact of fire has significantly transformed the soils of many of the Earth's natural zones (Li et al. 2021; Nelson et al. 2021). Fires are also an important geochemical factor that enhances the fluxes of elements from a catchment into rivers (Parham et al. 2013; Kuzmina et al. 2022; Kuzmina et al. 2024), and can reduce ecosystem productivity over long periods of time by reducing nitrogen stocks (Pellegrini et al. 2018). At the same time, the residual effect of fire on ecosystem processes persists for a long time not only due to interruption of successional development, destruction of litter, and leaching of chemicals elements (Cancelo-González et al. 2013), but also due to the penetration of charcoal on the soil surface (Luo et al. 2016), which has important ecological functions in boreal ecosystems (Hart and Luckai 2013). In subarctic ecosystems, fires can increase biodiversity for several decades (Heim et al. 2021).

Fire will become increasingly important in landscape dynamics due to current and near future climate warming (Kharuk et al. 2022; Mekonnen et al. 2022; Talucci et al. 2022). Fire dynamics in the boreal and subarctic regions are of particular concern, (Glückler et al. 2024; Shestakova et al., 2024), on the one hand because of high carbon stocks in vegetation and peat soil horizons, which is released into the atmosphere during fires (Nurrohman et al. 2024), and on the other hand because of the impact of fires on permafrost stability (Chen et al. 2021; Filimonenko et al. 2024). In order to make correct forecasts of the future impact of fires on ecosystems, it is necessary to refer to a distant retrospective, up to covering the entire Holocene and the previous warm and dry epochs. For these and other reasons, an increasing number of researchers are addressing fire dynamics in the Subarctic (Heim et al. 2022). However, there is still a long way to go before these issues are evenly studied in different regions of permafrost distribution (Heijmans et al. 2022). This way the Subarctic of North America and Europe is much better studied (Vachula et al. 2020; Scholten et al. 2024). The most studied in Russia in terms of reconstruction of paleofire dynamics are the central and southern parts of the East European Plain, as well as the south-east of Western Siberia (Pupysheva and Blyakharchuk 2023). The territory of Siberia is still being studied more by remote sensing, in the aspect of fire activity for the short-term retrospective.

One of the Siberian regions sensitive to landscape fire activity is Western Siberia due to the high rate in permafrost peatlands (Vasil'chuk and Vasil'chuk 2016). With regard to the study of paleofire activity in Western Siberia, its boreal part has been mainly investigated. In pioneering reseearch, charcoal layers in peat deposits were counted (Turunen et al. 2001) and periods of high fire activity were dated. In the last decade, work has been carried out to study the proxies of landscape fires in soils, peat and lake deposits of boreal landscapes of Western Siberia (Lamentowicz et al. 2015; Amon et al. 2020; Feurdean et al. 2022; Loiko et al. 2022; Startsev et al. 2022;

Blyakharchuk et al. 2024; Pupysheva and Blyakharchuk 2024; etc.). There is currently little information on the paleofire dynamics of subarctic permafrost landscapes in Western Siberia (Shefer et al. 2023), although in a number of interfluves, almost all landscapes have been affected by fires, and in relatively recent times (Moskovchenko et al. 2020; Sizov et al. 2021). All this emphasizes the importance of studying paleofire activity in the permafrost zone in the Holocene and identifying the causes of its fluctuations.

In this paper, we have studied the paleofire history in one of the typical low-tundra regions of Western Siberia using several proxies. The northern part of the Pur-Taz interfluve of the Yamal-Gydan ecoregion was chosen as such a region. The choice of this area is related not only to its good transport accessibility, but also to its location near the large Taz River, along which the presence of large settlements (Tazovsky factoria, Mangazeya town) has been known for several centuries even according to written sources.

This study combines paleofire data from both peat deposits of frozen polygonal peat plateaus and mineral soils located near peat plateaus. This is the first time that these different types of charcoal proxies have been compared for the Yamalo-Gydan ecoregion. Plant macrofossils and pollen in the peat that have had very limited peat growth in the last four thousand years have been previously investigated in this region (Pastukhov et al. 2021). In the present study, not only such a peat deposit was used, but also peat deposits that have had a marked increase in the last four thousand years, allowing a higher resolution for the second half of the Holocene for the distribution of charcoal in peat.

Materials and methods

Study area

The tundra ecosystems of the Pur-Taz interfluve are located in the continuous permafrost region, in the southern tundra subzone of Western Siberia (Zarov et al. 2021). The studied key area (Fig. 1) is located in the northeast of the Pur-Taz interfluve, within the third lacustrine-alluvial plain. Ridges, thermokarst-erosional hollows and basins of drained thermokarst lakes are common within this terrace (Loiko et al. 2020; Opokina et al. 2024). The studied part of the interfluve has a large area of permafrost polygonal peat plateaus, and the soils are mostly of loamy texture (Zarov et al. 2021). Active peat accumulation in this area began in the early Holocene (Tikhonravova et al. 2023) and is thought to have slowed significantly in the late Holocene, and permafrost polygonal peat plateaus are defined as relict (Fotiev 2017). Their microtopography is represented by alternating elevations (polygons), elongated interpolygonal depressions (cracks), and fens through which suprapermafrost water flows into streams (Loiko et al. 2019).

According to observations from the nearest meteorological station in the village of Tazovsky (67°28′ N; 78°44′ E) for 1991-2021, the average temperature of the coldest month (January) is -25.4 °C, the warmest month (July) is +14.4 °C, and the average annual temperature is -6.8 °C. The average annual precipitation reaches 515 mm (Climate data for cities around the world url: https://ru.climate-data.org/).
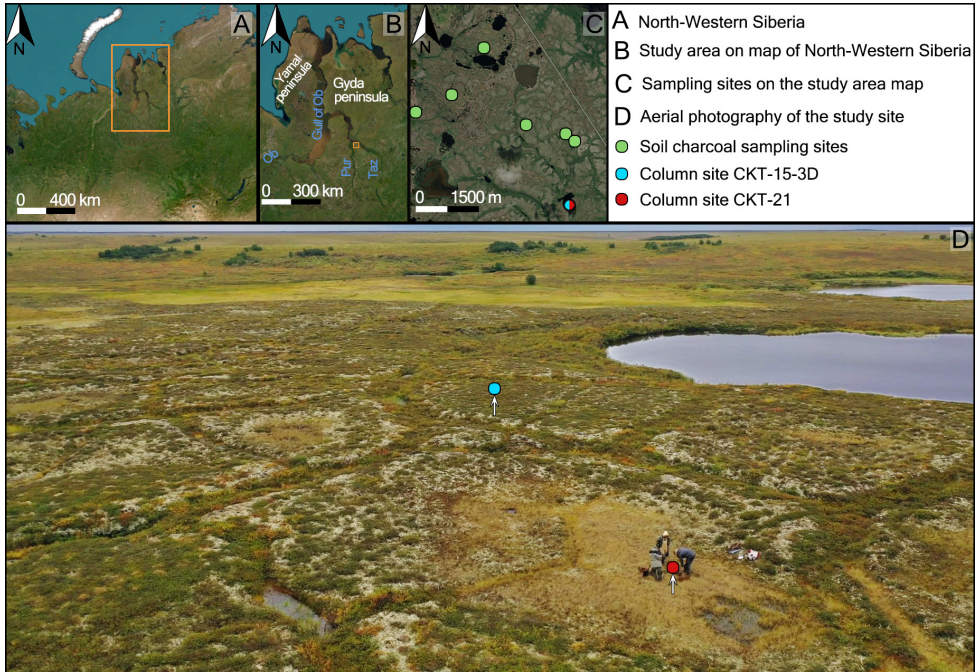

Figure 1. Maps and locations of the study sites.

The plant communities of the upland tundra are represented by moss-sedge-lichen tundra in the upper parts of the slopes and willow-dwarf birch-moss communities at the foot of the slopes. On the convex upper parts of the slopes, alder bushes with tundra meadows in the centre are found in places (Loiko et al. 2022). Single larch trees are rare. Peatland vegetation is widespread in extensive thermokarst depressions, ancient drained basins of thermokarst lakes, thermokarst-erosional hollows. Shrub-lichen and sedge-sphagnum communities occur on polygons of permafrost peat plateaus. In fens and cracks are cotton grass-sedge-sphagnum. Tall thickets of alder and willow grow in the floodplains along the rivers, with occasional larch, birch (Loiko et al. 2023). Highly productive grass communities grow under the cover of trees and shrubs.

Fieldwork

Fieldwork was carried out during the summers of 2015–2021, during which time two cores were collected from the central parts of adjacent polygonal bog polygons and a series of soil charcoal. The peat core CKT-15-3D (400 cm) was collected in 2015 by geological core drilling using the UKB-12/25-01 rotary drilling rig (Russia, Yekaterinburg, 'Machine-Building factory V. V. Vorovsky' LLC) with a compartment length of one metre and a diameter of 59 mm. After drilling, the column was cut into 2.5 cm thick samples which were packed in hermetic bags and frozen. Peat core CKT-21 (48 cm) was sampled in 2021 as a monolith (Fig. 1). The column was later cut into 1 cm thick samples which were packed into hermetic bags and frozen. To describe the morphology of mineral and peat soils, the International Soil Classification System WRB (IUSS... 2022) was used.

Charcoal was collected from the soil pits by extracting it from the front wall, which had been cleared with a shovel. Charcoal larger than 2 mm in size, easily visible to the naked eye, was collected. All charcoal that was found in the range from the mineral surface of the soil to the soil-forming deposit or permafrost was collected. No charcoal was collected from under the plant litter, i.e. from the mineral surface of the soil. All the soils from which the charcoal were collected were mineral and were located either on tundra upland plains or in the basins of drained thermokarst lakes. Charcoal in tundra soils are small in size, as they are usually formed from dwarf shrubs. They are scattered, as they are immersed in the soil during cryoturbation. They are often sealed in dense loam and are destroyed during extraction. Therefore, all more or less large undestroyed charcoal was selected. If charcoal formed a cluster in the form of a morphon (patch), then the largest charcoal from this patch was selected. In general, the methodology for extracting soil charcoal and its subsequent preparation for radiocarbon dating was completely analogous to previous works (Bobrovsky et al. 2019; Loiko et al. 2022).

Radiocarbon dating and age-depth modelling

Radiocarbon analysis of peat using liquid scintillation spectrometry was carried out at the Kiev Radiocarbon Laboratory, Ukraine (7 samples, index Ki) and the Institute of Monitoring of Climatic and Ecological Systems, SB RAS, Russia (3 samples, index IMCES). Radiocarbon analysis using accelerator mass spectrometry was carried out at the Poznań Radiocarbon Laboratory, Poland (10 samples, index Poz), the National Taiwan University AMS Lab Taiwan (2 samples, index NTUAMS). Preparing for radiocarbon dating of plant remains samples with IGANAMS index (1 sample) was carried out at the Laboratory of Radiocarbon Dating and Electron Microscopy of the Institute of Geography of the Russian Academy of Sciences (Moscow) and radiocarbon analysis using accelerator mass spectrometry was carried out at the Isotope Research Centre of the University of Georgia (USA). Calibration of the radiocarbon

age in the calendar was carried out at the OxCal 4.4. program using IntCal20 calibration curve (Reimer et al. 2020). Errors are expressed at the two sigma level of confidence, and dates are quoted in calendric years BP (Tables 1, 2).

Table 1. Radiocarbon dating for soil charcoal used in this study

Lab. code	Depth (cm)	Material	^{14}C date (yr BP, 2σ)	Calibrated age (cal. yr BP, 2σ)	Location (lat., long.)
Poz-120345	40	Charcoal	305 ± 30	388 ± 47	N67.36981°, E78.70874°
Poz-121689	26	Charcoal	850 ± 30	747 ± 39	N67.37308702°, E78.68130051°
Poz-120331	15	Charcoal	925 ± 30	844 ± 46	N67.37605000°, E78.61897000°
Poz-114028	18	Charcoal	930 ± 30	846 ± 44	N67.37975953°, E78.63923543°
Poz-121690	68	Charcoal	2445 ± 30	2497 ± 105	N67.37308702°, E78.68130051°
Poz-120317	40	Charcoal	2445 ± 30	2505 ± 105	N67.36981°, E78.70874°
Poz-114031	21	Charcoal	6885 ± 35	7715 ± 41	N67.38977000°, E78.65852000°
Poz-120332	30	Charcoal	7120 ± 40	7948 ± 44	N67.36991°, E78.709°
Poz-120334	20	Charcoal	7250 ± 50	8080 ± 61	N67.36991°, E78.709°
IGANAMS-6115	50	Charcoal	1360 ± 20	1291 ± 22	N67.37308702°, E78.68130051°
NTUAMS-8728	80	Charcoal	9168 ± 111	10361 ± 135	N67.37308702°, E78.70319444°

An age-depth models was established using "rbacon" package in R (Blaauw and Christen 2011) and IntCal20 calibration curve. Dating obtained for samples at depths of 275–277.5 cm and 320–322.5 cm is unreliable, in the model they are marked as "outlier". Age-depth model for the sediment core (CKT-15-3D) suggest that the sediment covers 11.2 cal kyr BP and lack of sedimentation between 4.4 and 0.8 cal kyr BP (Fig. 3). The upper part of the sediment (0–20 cm) started to accumulate recently.

Table 2. Radiocarbon dating for columns used in this study

Lab. code	Depth (cm)	Material	^{14}C date (yr BP, 2σ)	Calibrated age (cal. yr BP, 95.4 % probability)	Modeled age (cal. yr BP)
CKT-15-3D					
Ki-20118	7.5–10	Peat	104,6% ± 0.9% pMC	Recent	50
Ki-20119	37.5–40	Peat	4510 ± 50	5159 ± 94	4903
Ki-20120	132.5–135	Peat	5410 ± 90	6194 ± 107	6148
Ki-20121	152.5–155	Peat	5580 ± 90	6375 ± 94	6364
Ki-20123	275–277.5	Peat	600 ± 300	589 ± 279*	7967
Ki-20122	290–292.5	Peat	7310 ± 80	8117 ± 89	8170
Ki-20124	320–322.5	Peat	6980 ± 140	7812 ± 127	8960
Poz-83157	342.5–345	Plant remains	9100 ± 50	10253 ± 64	10037

Lab. code	Depth (cm)	Material	¹⁴C date (yr BP, 2σ)	Calibrated age (cal. yr BP, 95.4 % probability)	Modeled age (cal. yr BP)
			CKT-21		
IMCES-14C2851	9–10	Peat	1205 ± 85	1124 ± 93	1048
IMCES-14C2850	27–28	Peat	2360 ± 95	2428 ± 155	2379
IMCES-14C2849	36–37	Peat	2755 ± 95	2877 ± 110	2869
NTUAMS-8726-1	45	Plant remains	3026 ± 100	3208 ± 110	3275

Laboratory analyses

We divide a charcoal particles into micro-charcoal (DM > 10 μm, where DM is the maximum dimension of the particle) and macro-charcoal (DM > 125 μm) particles.

Micro-charcoal analysis

Samples for analysis (~1 cm³) were taken throughout the thickness of peat sediments every 1 cm for column CKT-21 and every 2.5–22.5 cm for column CLT-15-3D. Samples were treated according to palynological methodology (Erdtman 1943), using acetolysis. One tablet of Lycopodium clavatum spores was initially added to each weighted sample as a reference for concentration calculation (Stockmarr 1971). For the CKT-15-3D column material, we used tablets with batch numbers 1031 and 3862 (containing 20848 ± 1546 and 9666 ± 212 spores, respectively). For the CKT-21 column material, we used only tablets with batch number 3862. CKT-15-3D column material from depths of 320 cm and below contained silicates and was treated with HF for 24 hours.

Micro-charcoal and non-pollen palynomorphs (NPP) were counted using a Zeiss Axiolab A1 microscope at 400× and 1000× magnification. Identification of NPPs was carried out using database NPP-ID (Shumilovskikh et al. 2022a; Shumilovskikh et all. 2022b).

The following formula was used to calculate the micro-charcoal concentration (M) per cm³:

$$M = C * Lyc^t / Lyc^l, \qquad (1)$$

where:
C – the identified number of micro-charcoal;
Lyc^l – the identified number of Lycopodium spores;
Lyc^t – the number of Lycopodium spores in tablet.

Macro-charcoal analysis

Samples for analysis (~2 cm³) are taken throughout the thickness of peat sediments every 1 cm. Standard sample processing technique is used for macro-charcoal analysis (Whitlock and Larsen 2001; Mooney and Tinner 2011) with using a 10% solution of KOH and 6% solution of H_2O_2. Macro-charcoal was counted with a "Zeiss Axio Zoom.V16" microscope at 45× magnification using a Bogorov's camera to count the total number of macro-charcoal. The statistical processing of the obtained data on the concentration of macro-charcoal in sediments is carried out in the "CharAnalysis" adapted for the "R" program (Higuera 2009). The number of macro-charcoal particles, their depth, and the upper and lower limits of their age (by age-depth model), served as the initial data for analysis.

Statistical interpretation of the data was carried out in several steps similar to the articles by Kupriyanov and Novenko (Kupriyanov and Novenko 2019):

1.   Based on the obtained concentration values, the rate of macrocharcoal accumulation was calculated. Concentration values, sampling depth, and age were interpolated to bring them to a single time resolution of 70 years, the median time resolution of the selected samples calculated on the basis of the Age-depth model;

2.   Background values of charcoal accumulation rate were calculated to smooth short-period fluctuations and subsequent separation of local and regional signals. We chose the Locally Estimated Scatterplot Smoothing (LOESS) regression method with a smoothing interval of 400 years, which best described the charcoal particle accumulation curve to identify the background values;

3.   To identify local pyrogenic events, a threshold value was calculated assuming that the 'noises' are distributed according to the Gaussian model of impurity dispersion within a user-defined time window. The Signal-to-Noise Index (SNI) was applied for each time window to assess statistical validity. To unify the statistical functions, we used a window resolution of 3300 years, the range of SNI values was from 2 to 5, which satisfies the statistical requirements of the analysis. We set the 95th percentile of the noise distribution as the threshold. If the determined values of coal accumulation rate were higher than this threshold, it was classified as a reliable local fire event.

Results

Dating for soil charcoal

The results of soil charcoal dating are summarised in Table 1. Figure 2 shows examples of localisation of dated charcoal in relation to patches composing the morphological pattern of the soil profile. This figure shows that depth in mineral soils does not affect the age of the charcoal as it usually does in peat soils. Charcoal more than 8 cal kyr BP old can be as little as 10 cm below the mineral soil surface, while charcoal about 2.5 cal kyr BP can be at 60–70 cm deep.

Figure 3 shows a ranked series of charcoal dates. The dates are grouped into three areas, two of which are confined to the Early Holocene and two to the Late Holocene. The largest number of charcoal dates are from the last 2.5 thousand years. Between 8 and 3 thousand years is a large time interval without dates. The charcoal with the oldest date to be 10366±133 cal yr BP and sampled from a depth of 80 cm. In this case it is confined to an ancient humus structure of dark grey colour, which arose on the site of a melted ice wedge during the Holocene climate warming, which occurred not earlier than the considered date.
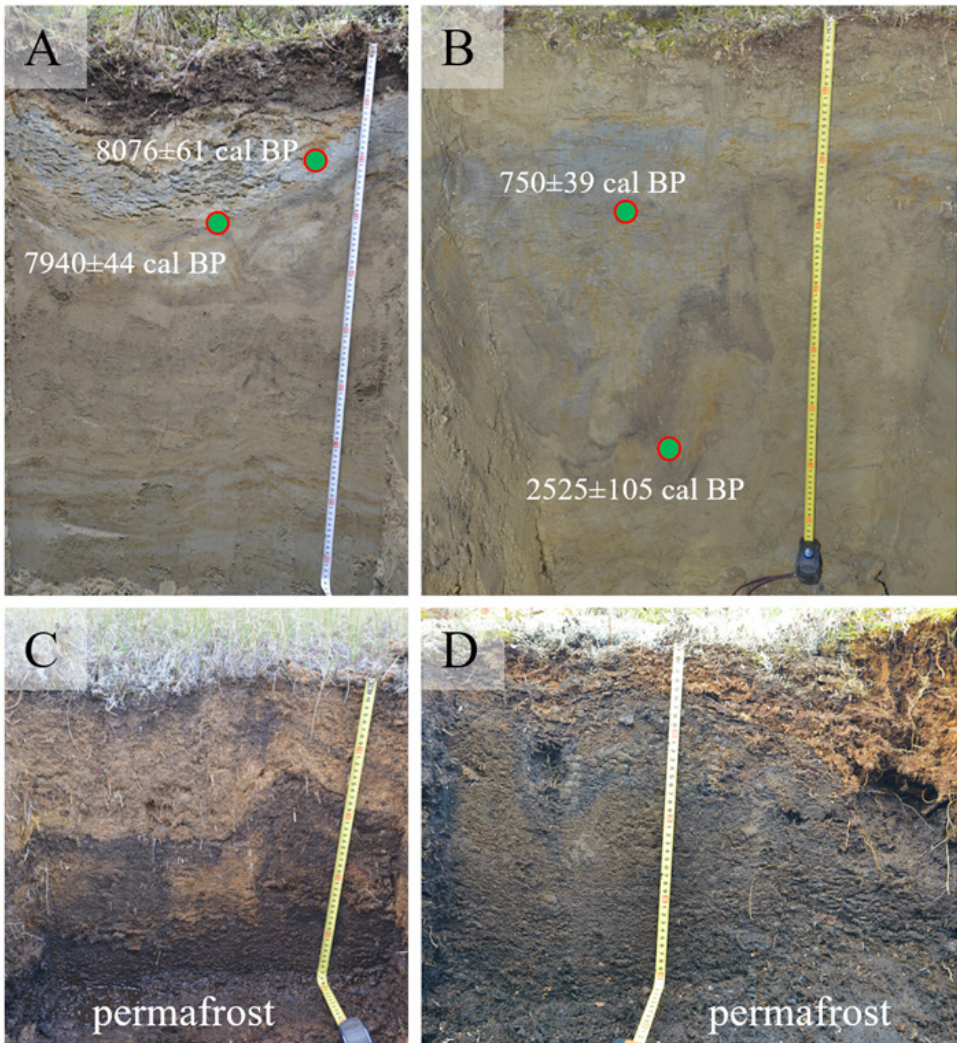
Figure 2. Examples of soils studied and locations of dated charcoal: A – Gleyic Cryosol at the foot of a slope; B – Gleyic Cryosol at the summit of a slope; C – Cryic Epifibric Endohemic Histosol in a depression on a polygon of the peat plateau; D – Hemic Cryic Histosol on a polygon of the peat plateau.
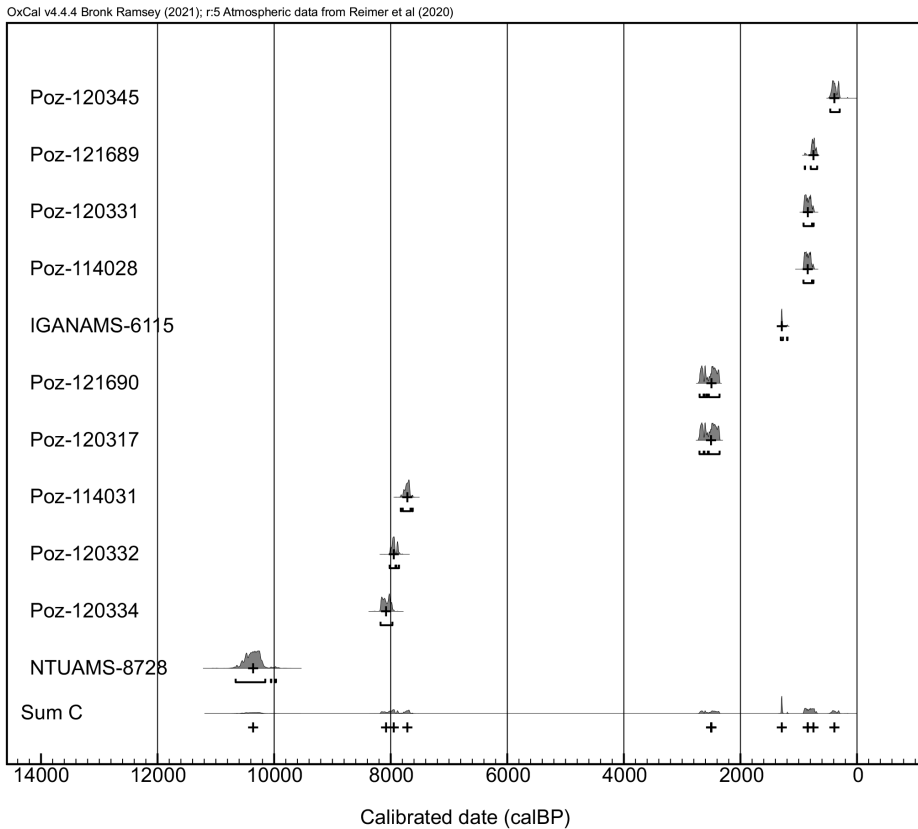
OxCal v4.4.4 Bronk Ramsey (2021); r:5 Atmospheric data from Reimer et al (2020)

Figure 3. Calibrated dates of soil charcoal.

Age-depth models of peat deposits of polygonal permafrost peat plateaus

The peat deposit of the studied peat plateau is about 340 cm deep, with lake sediments below it, which were drilled to a depth of 400 cm. The highest intensity of peat accumulation was during the period from 8 to 5.5 cal kyr BP. Thereafter, the intensity of peat accumulation generally decreased and became highly variable depending on the microtopography. Thus, on polygons with convex center it almost ceased and for about 5 thousand years it was no more than 25 cm (Fig. 4). At the same time, polygons with concave center accumulated 48 cm of peat over a period of 3.5 thousand years.

Peat accumulation rates in profile CKT-21 slowed throughout the studied period, especially from 2.3 cal kyr BP (Fig. 4A). These differences in peat accumulation rates are also reflected in the morphology of the peat soils. Thus, in the CKT-21 profile, the upper 20 cm of peat has a predominantly sedge and sphagnum composition of plant macrofossils (Fig. 2C, D). This horizon is diagnosed as Oi. At the same time, in the upper 20 cm of profile CKT-15-3D the peat consists of macrofossils of

shrubs, lichens and green mosses. This horizon is diagnosed as Oe. Thickness of the active layer also differs, in profile CKT-21 it is 10–15 cm more.

Micro-charcoal and NPP

The full CKT-15-3D column contain 400 cm and consist of lake sediment (400–340 cm) and peat sediment (340–0 cm). The concentration of microcharcoal at lake sediment part (11.2–9.7 cal kyr BP) is quite high (56K–230K particles). The peat sediments of core CKT-15-3D can be divided into 2 periods based on the number of micro-charcoal. The period 11.2–8 cal kyr BP, for which a high concentration of micro-charcoal (1.3K–806K particles) and the period 8–4.4 cal kyr BP, for which a low concentration of micro-charcoal (1.3K–19K particles) is noted. The spores of *Gelasinospora* are presence at: 11.2, 10.7, 10.6, 9, 8.2, 8.1, 7.7, 5.4 cal kyr BP. The spores of *Glomus* are presence at: 11.2, 8.9, 8.3, 8.1, 8, 7.9, 6.7, 6.4, 4.9 cal kyr BP (Fig. 5A).

The 48 cm column CKT-21 is divided into four periods. Period 3.4–3 cal kyr BP, a minimum concentration of charcoal (8K–22K particles) is noted. In the period 3–2.3 cal kyr BP, the concentration of charcoal increases, ranging from 25K–88K particles. The maximum charcoal concentration is during the period 2.3–1.1 cal kyr BP (20K–106K charcoal particles). Around 1.1 cal kyr BP, the concentration of micro-charcoal decreases and during the period 1.1–0 cal kyr BP makes 2K–31K particles. The spores of *Gelasinospora* is presence at: 2.9, 2.8, 2.6, 2.5, 2.4, 2.3, 2.2, 1.8, 1.7, 1.5, 1.4, 1.2, 1.1, 1 cal kyr BP, ~251 cal yr BP and ~24 cal yr BP. The spores of *Glomus* are presence at: 3.4, 3.3, 2.6, 2.4, 2.3, 2.2, 1.8, 1.5, 1.2, 1, 0.8 and 0.5 cal kyr BP (Fig. 5B).
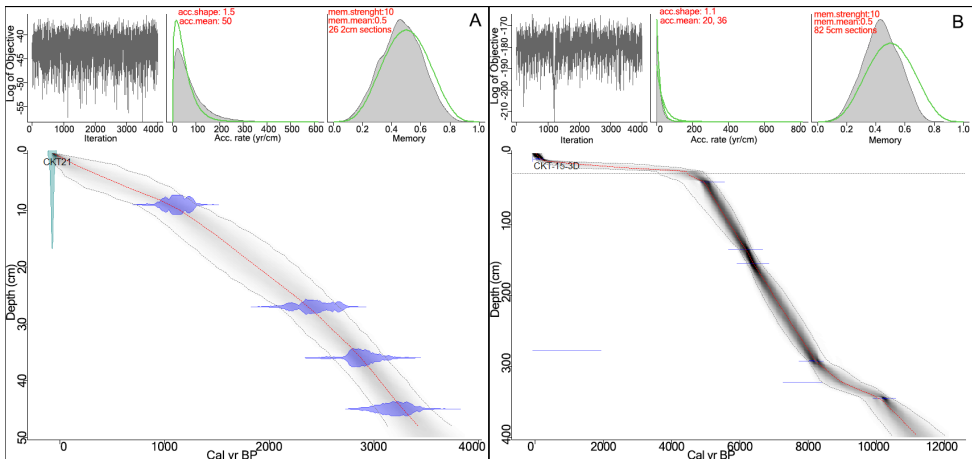

Figure 4. Bacon age-depth models for (A) column CKT-21 and (B) CKT-15-3D. Calibrated 14C AMS dates are shown in transparent blue, and the age-depth model is shown in grey (darker greys indicate more likely calendar ages; grey dashed lines show 95% confidence intervals).

Macro-charcoal

Results of macro-charcoal accumulation rate calculations obtained using the CharA-nalysis software show the dynamics of local fires, over ~3.5 cal kyr BP (Fig. 6).

Background char accumulation rates ranged from 0.1 to 4.2 char particles per cm^2/yr (c. p. per cm^2/yr). The three events with the highest charcoal accumulation rates were observed between ~2.2 cal kyr BP and 3–2.3 cal kyr BP (4.2 c. p. per cm^2/yr), 2.6 cal kyr BP (3.1 c. p. per cm^2/yr), and 2.9 cal kyr BP (3.8 c. p. per cm^2/yr). The minimum background accumulation rate was observed between ~0 and 0.8 cal kyr BP (0.1–0.6 c. p. per cm^2/yr). CharAnalysis interpretation of fire events recorded 13 local fire episodes (Fig. 5): 0.6, 1.1, 1.2, 1.3, 1.5, 1.6, 2, 2.3, 2., 2.6, 2.7, 2.9 and 3.2 cal kyr BP.
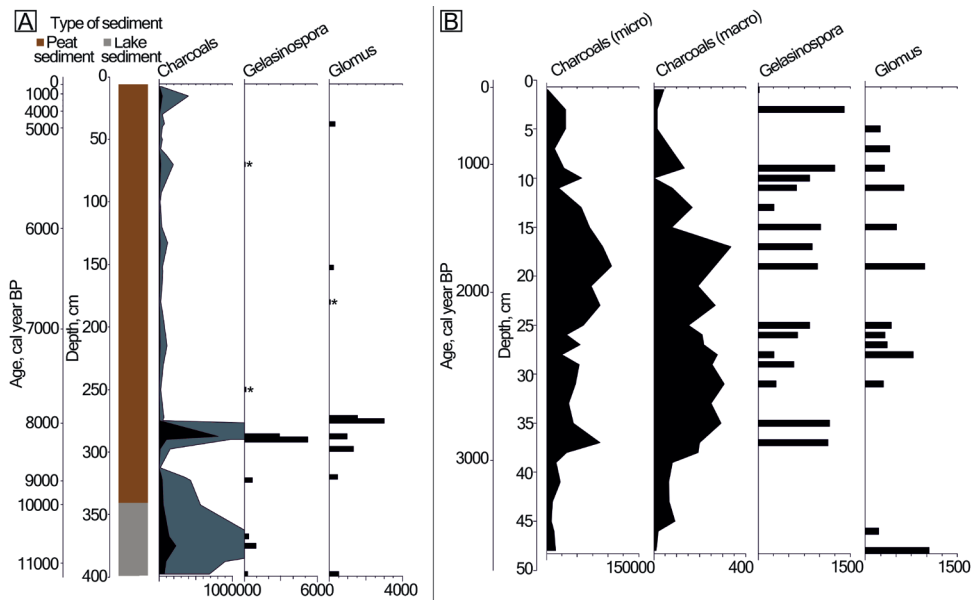

Figure 5. Charcoal and non-pollen palynomorphs for columns CKT-15-3D(A) and CKT-21(B).

Discussion

Our complex study of five terrestrial paleofire proxies for the landscapes of the Pur-Taz interfluve is the first such work for the Yamal-Gydan ecoregion. Charcoal in peat appears not only due to fires in the peatlands itself, but also due to wind-borne input from the surrounding upland landscapes. The study of charcoal in the soils (Figs 2, 7) of the latter allowed the two archives to be compared. Such research has never been carried out before, not only in the region under study, but also in the

whole of Western Siberia. In this connection, some features of the location of char-coal in soils should be considered.

We identified four main types of charcoal transport mechanisms in mineral soils. (1) Transport by cryoturbation (Fig. 2B). This process is more characteristic of the thixotropically patterned summit slope of an upland tundra. (2) Charcoal deposition in a microtopographic depression following fire, activating erosion processes (Fig. 7A). (3) Charcoal deposition as a result of melting of ice veins in the first half of the Holocene during climate warming (Fig. 7B). (4) Transfer of charcoal to thermokarst lakes by coastal abrasion, its deposition on the bottom with subsequent accumulation of peat after lake drainage (Fig. 7C).
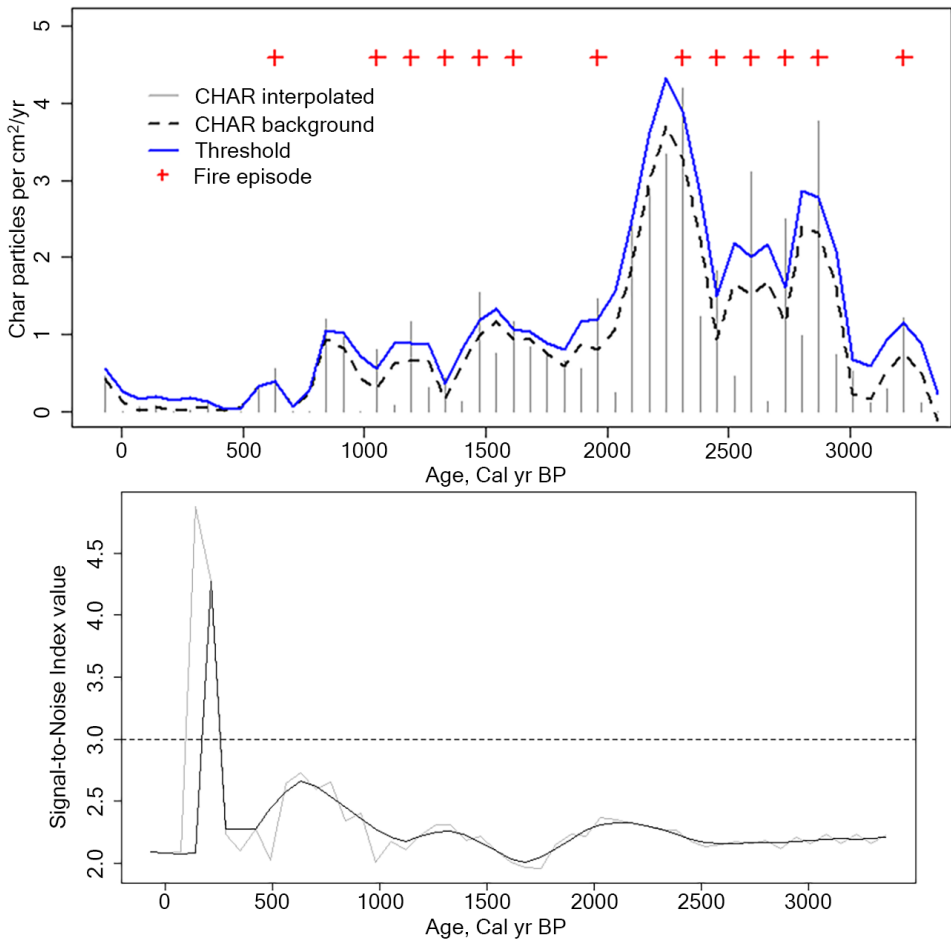

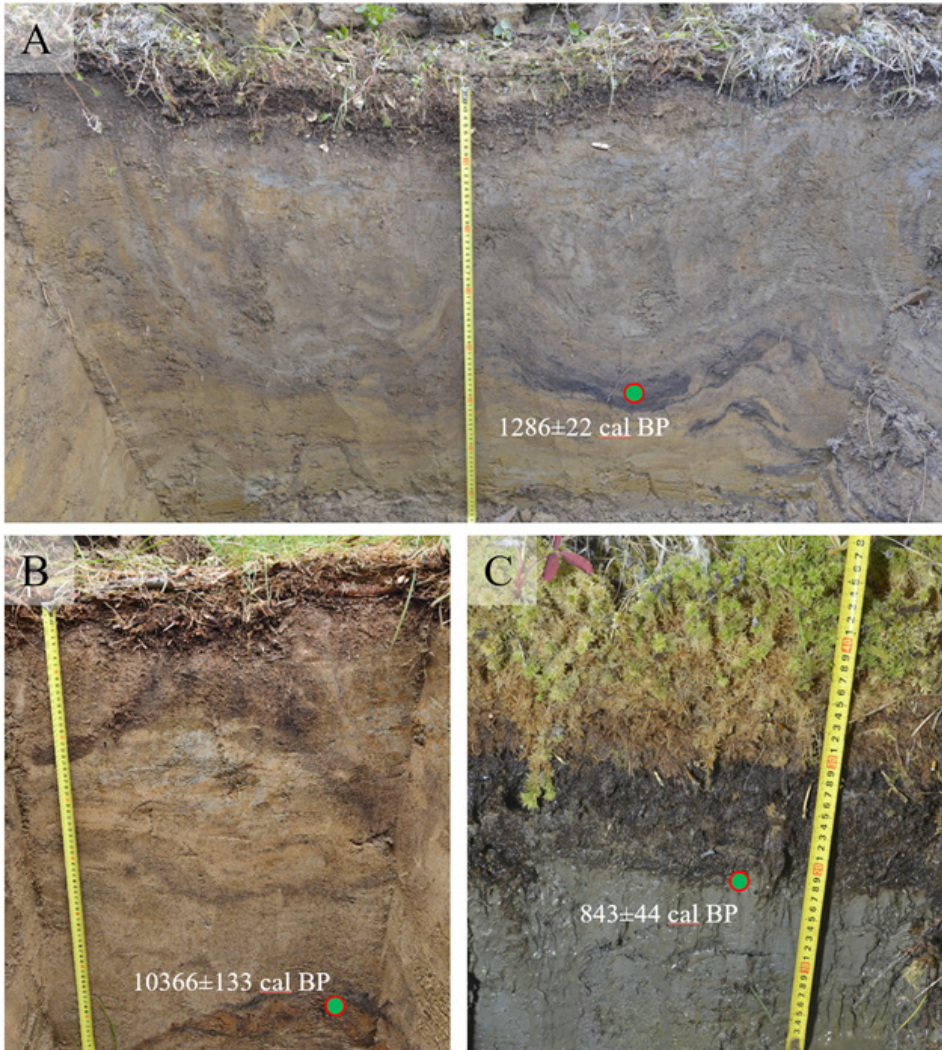**Figure 6.** Local fire frequency for column CKT-21.

Figure 7. Examples of soils studied and locations of dated charcoal: A – Gleyic Cryosol; B – Gleyic Cryosol (Ochric); C – Histic Gleysol (Gelic).

Analyses of charcoal dates show that relatively young charcoal (less than 2,000 years old) can be found at rather deeper depths (more than 50 cm). This is associated with active cryoturbation in the areas of thixotropically patterned ground. This weakly depth-dependent distribution of radiocarbon dates is similar to the distribution of the age of organic matter in the profile of cryogenic soils, for which relatively young radiocarbon dates have also been recorded at deep depths (Palmtag et al. 2015). Cryoturbations lead to inversion of radiocarbon dates in peat deposits as well, which is well known (Pastukhov et al. 2021; Tikhonravova et al. 2023).

However, there are also cases of ancient dates located near the surface (see Fig. 2A). Such soils are found at the foot of slopes, where the soil is more stable due to the organogenic horizon.

The presence of charcoal of about 8 thousand cal. yr BP in the surface horizons of Gleyic Cryosol indicates that permafrost soils protect charcoal from decomposition. Earlier it was stated that charcoal in soil can be completely decomposed in 4–5 thousand years (Kuzyakov et al. 2014). Obviously, under conditions of permafrost and gleyisation, charcoal decomposes much more slowly. Cryosols can be considered a good archive of paleofires. These soils provide not only high spatial resolution, but also high temporal resolution.

The *Gelasinospora* and *Glomus* fungi used in this work have not been previously used for the tundra of Western Siberia. Therefore, when interpreting the fact of their presence in a peat deposit, it is necessary to take into account some features of the tundra environment. For example, the fungus *Gelasinospora* is considered to be carbonicolous, which means that it grows on both burnt soil and burnt wood (Lageard and Ryan 2013; Stivrins et al. 2019), and the fungus *Glomus* grows on open eroded soil (Van Geel et al. 2011). In the boreal region, a significant part of the communities are woodlands, whereas in the tundra, the woody biomass that is able to burn is much lower. Therefore, in the tundra, the number of *Gelasinospora* spores will be strongly dependent on the proportion of shrubs and dwarf shrubs and will be significantly lower compared to similar spectra in boreal regions. And *Glomus* spores can probably form in the tundra not only after post-pyrogenic erosion, but also without fires at all, during cold periods, when solifluction and patterned ground formation processes are activated. It is therefore possible that *Glomus* spores are not always associated with other proxies.

To discuss the fire history in the region, we collected all the proxy data used in the study. Microcharcoal, which records more regional fires. Macrocharcoal, soil charcoal, and fungal spores, which record local fires. Given the different resolution of the CKT-15-3D and CKT-21 cores, we visualized the results with a time resolution of 500 years for a more relevant presentation of the results in Fig. 8.
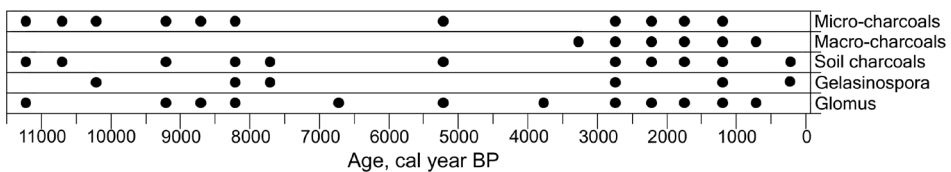

Figure 8. Indicators of fire events for the last 11.2 cal kyr BP.

We identified three time periods that reflect millennial changes in fire activity. In the first period from 11.2 to 7.5 cal kyr BP, high fire activity was recorded. In the second period from 7.5 to 3.5 cal kyr BP the number of fire events is minimal. In the third period from 3.5 cal kyr BP to the present day, the number of pyrogenic events

is maximum, and the maximum occurs in the second and third millennia from our days.

Fire events of the first period are recorded in all proxy types. High fire activity at the beginning of the Holocene has previously been reported for the study area (Peteet et al. 1998), and our data confirm this. The most intense fires occurred immediately after the 8.2 cal kyr BP event. This event has been associated with climate cooling (Zhao et al. 2022), but it is currently difficult to assess the mechanism of fire occurrence after this cooling.

In the second period, only one fire was recorded, which occurred 5.4 cal kyr BP. Also, the appearance of *Glomus* spores was noted for this period, in the absence of other proxies, which may be associated with deflationary processes. A decrease in the frequency of fires during this period is consistent with data for the middle taiga of Western Siberia (Loiko et al. 2022, Pupysheva and Blyakharchuk 2024). In contrast, for north Yenisei Siberia has a significant frequency of fire events during the periods 6.3-5.8 cal kyr BP (Novenko et al. 2023). There are other regions of the Arctic that experienced a significant number of fire events during this period. In the southeast of the Kola Peninsula, for example, at least 12 fire events were recorded between 7000 and 5000 cal BP (Mergelov et al. 2024).

The third period is characterised by the highest fire frequency. In published studies for the studied region, this period is the one with the least data, as peat deposits with extremely slow (or interrupted) peat accumulation were analysed during this period (Peteet et al. 1998; Tikhonravova et al. 2023; Pastukhov et al. 2021). The peat deposit with active peat accumulation in the second half of the Holocene selected in our work, as well as the use of soil charcoal dating, made it possible to record high fire activity during this period. Similar results have been obtained for the middle taiga (Loiko et al. 2022; Pupysheva and Blyakharchuk 2024) and for Putorana Plateau (Novenko et al. 2022). Since this period was not the driest, we can assume the influence of ancient anthropogenic activities. There are archaeological sites a few kilometers from the field site. We know of settlements that existed in the second half of the fourth millennium, the middle of the second millennium and the beginning of the first millennium. For the last five hundred years there have been Russian settlements in the lower reaches of the Taz River (Stepanova and Syuzyumov 2019; Tkachev and Tkachev 2019; Tkachev 2018). A similar relationship between fire frequency and features of archaeological cultures has been noted previously for the southwest of Western Siberia (Ryabogina et al. 2024).

Conclusion

The study is the first to compare different landscape paleofire proxies with very different recording mechanisms. This allowed information on fire activity to be obtained for almost the entire Holocene. The work demonstrates the prospects of such

an approach, due to which the records of peat columns of large peat depressions and soils of upland plains complement each other.

For paleoecological studies in the Yamalo-Gydan ecoregion, the analysis of peat deposits of concave polygons of permafrost peat plateaus turned out to be very promising. In these polygons, peat accumulation has been uninterrupted for the last four millennia.

The mechanisms of charcoal transfer to soils are considered. Charcoal transfer in mineral soils depends strongly on the microtopographic position of the soil profile. Under the influence of suprapermafrost water with the formation of a peat horizon, the intensity of cryoturbation decreases. Ancient charcoal may occur near the mineral surface. In soils with the highest cryoturbation activity, young charcoal often occurs at depth.

Three periods with different frequencies of fire events were identified. According to the generalised data, the number of fire events was estimated for intervals of 0.5 millennia. The frequency of pyrogenic events in these periods was determined by both climatic events and ancient human influence.

Acknowledgement

References

Amon L, Blaus A, Alliksaar T, Heinsalu A, Lapshina E, Liiv M, Reitalu T, Vassiljev J, Veski S (2020) Postglacial flooding and vegetation history on the Ob River terrace, central Western Siberia based on the palaeoecological record from Lake Svetlenkoye. Holocene 30(5): 618–631. https://doi.org/10.1177/0959683619895582

Blaauw M, Christen JA (2011) Flexible Paleoclimate age-depth models using an Autoregressive Gamma Process. Bayesian Analysis 6(3): 457–474. https://doi.org/10.1214/11-ba618

Blyakharchuk TA, van Hardenbroek M, Pupysheva MA, Kirpotin SN, Blyakharchuk PA, (2024) Late Glacial and Holocene history of climate, vegetation landscapes and fires in South Taiga of Western Siberia based on radiocarbon dating and multi-proxy palaeoecological research of sediments from Shchuchye Lake. Radiocarbon:1–24. https://doi.org/10.1017/RDC.2024.103

Bobrovsky MV, Kupriaynov DA, Khanina LG (2019) Anthracological and morphological analysis of soils for the reconstruction of the forest ecosystem history (Meshchera

Lowlands, Russia). Quaternary International 516: 70–82. https://doi.org/10.1016/j.quaint.2018.06.033

Cancelo-González J, Rial-Rivas ME, Díaz-Fierros F (2013) Effects of fire on cation content in water: A laboratory simulation study. International Journal of Wildland Fire 22(5): 667–680. https://doi.org/10.1071/WF12178

Certini G, Moya D, Lucas-Borja ME, Mastrolonardo G (2021) The impact of fire on soil-dwelling biota: A review. Forest Ecology and Management 488: 118989. https://doi.org/10.1016/j.foreco.2021.118989

Chen Y, Lara MJ, Jones BM, Frost GV, Hu FS (2021) Thermokarst acceleration in Arctic tundra driven by climate change and fire disturbance. One Earth 4(12): 1718–1729. https://doi.org/10.1016/j.oneear.2021.11.011

Climate data for cities around the world (2024) Internet resource. https://ru.climate-data.org (Accessed on 26.11.2024).

Erdtman G (1943) An introduction to pollen analysis. Chronica Botanica, Waltham, 239 pp.

Feurdean A, Diaconu A-C, Pfeiffer M, Gałka M, Hutchinson SM, Butiseaca G, Gorina N, Tonkov S, Niamir A, Tantau I, Zhang H, Kirpotin S (2022) Holocene wildfire regimes in western Siberia: interaction between peatland moisture conditions and the composition of plant functional types. Climate of the Past 18(6): 1255–1274. https://doi.org/10.5194/cp-18-1255-2022

Filimonenko E, Uporova M, Prikhodko N, Samokhina N, Belyanovskaya A, Kurganova I, Gerenyu VL, Merino C, Matus F, Chen C, Alharbi SA, Soromotin A, Kuzyakov Y (2024) Organic matter stability in forest-tundra soils after wildfire. Catena 243: 108155. https://doi.org/10.1016/j.catena.2024.108155

Fotiev SM (2017) Arctic peatlands of the Yamal-Gydan province of Western Siberia. Earth's Cryosphere 21: 3–13. https://doi.org/10.21782/EC1560-7496-2017-5(3-13)

Glückler R, Gloy J, Dietze E, Herzschuh U, Kruse S (2024) Simulating long-term wildfire impacts on boreal forest structure in Central Yakutia, Siberia, since the Last Glacial Maximum. Fire Ecology 20: 1. https://doi.org/10.1186/s42408-023-00238-8

Hart S, Luckai N (2013) REVIEW: Charcoal function and management in boreal ecosystems. Journal of Applied Ecology 50(5): 1197–1206. https://doi.org/10.1111/1365-2664.12136

Heijmans MM, Magnússon RÍ, Lara MJ, Frost GV, Myers-Smith IH, van Huissteden J, Jorgenson MT, Fedorov AN, Epstein HE, Lawrence DM, Limpens J (2022) Tundra vegetation change and impacts on permafrost. Nature Reviews Earth & Environment 3(1): 68–84. https://doi.org/10.1038/s43017-021-00233-0

Heim RJ, Bucharova A, Brodt L, Kamp J, Rieker D, Soromotin AV, Yurtaev A, Hölzel N (2021) Post-fire vegetation succession in the Siberian subarctic tundra over 45 years. Science of the Total Environment 760: 143425. https://doi.org/10.1016/j.scitotenv.2020.143425

Heim RJ, Heim W, Bültmann H, Kamp J, Rieker D, Yurtaev A, Hölzel N (2022) Fire disturbance promotes biodiversity of plants, lichens and birds in the Siberian subarctic tundra. Global Change Biology 28(3): 1048–1062. https://doi.org/10.1111/gcb.15963

Higuera PE (2009) CharAnalysis 0.9: Diagnostic and Analytical Tools for Sediment-Charcoal Analysis. User's Guide. https://www.researchgate.net/publication/254406379_CharAnalysis_09_Diagnostic_and_analytical_tools_for_sediment-charcoal_analysis (accessed on 1 December 2024).

IUSS Working Group WRB (2022) World Reference Base for Soil Resources. International soil classification system for naming soils and creating legends for soil maps. 4th edition. International Union of Soil Sciences (IUSS), Vienna, 236 pp.

Kelly LT, Giljohann KM, Duane A, Aquilué N, Archibald S, Batllori E, Bennett AF, Buckland ST, Canelles Q, Clarke MF, Fortin M-J, Hermoso V, Herrando S, Keane RE, Lake FK, McCarthy MA, Morán-Ordóñez A, Parr CL, Pausas JG, Penman TD, Regos A, Rumpff L, Santos JL, Smith AL, Syphard AD, Tingley MW, Brotons L (2020) Fire and biodiversity in the Anthropocene. Science 370(6519): eabb0355. https://doi.org/10.1126/science.abb0355

Kharuk VI, Dvinskaya ML, Im ST, Golyukov AS, Smith KT (2022) Wildfires in the Siberian Arctic. Fire 5(4): 106. https://doi.org/10.3390/fire5040106

Kupriyanov DA, Novenko EY (2019) Reconstruction of the Holocene Dynamics of Forest Fires in the Central Part of Meshcherskaya Lowlands According to Antracological Analysis. Contemporary Problems of Ecology 12(3): 204–212. https://doi.org/10.1134/S1995425519030065

Kuzmina D, Lim AG, Loiko SV, Pokrovsky OS (2022) Experimental assessment of tundra fire impact on element export and storage in permafrost peatlands. Science of the Total Environment 853: 158701. https://doi.org/10.1016/j.scitotenv.2022.158701

Kuzmina D, Loiko SV, Lim AG, Istigechev GI, Kulizhsky SP, Julien F, Rols JL, Pokrovsky OS (2024) Macro-and micronutrient release from ash and litter in permafrost-affected forest. Geoderma 447: 116925. https://doi.org/10.1016/j.geoderma.2024.116925

Kuzyakov Y, Bogomolova I, Glaser B (2014) Biochar stability in soil: decomposition during eight years and transformation as assessed by compound-specific 14C analysis. Soil Biology and Biochemistry 70: 229–236. https://doi.org/10.1016/j.soilbio.2013.12.021

Lageard JG, Ryan PA (2013) Microscopic fungi as subfossil woodland indicators. The Holocene 23(7): 990–1001. https://doi.org/10.1177/0959683612475145

Lamentowicz M, Słowiński M, Marcisz K, Zielińska M, Kaliszan K, Lapshina E, Gilbert D, Buttler A, Fiałkiewicz-Kozieł B, Jassey VEJ, Laggoun-Defarge F, Kołaczek P (2015) Hydrological dynamics and fire history of the last 1300 years in western Siberia reconstructed from a high-resolution, ombrotrophic peat archive. Quaternary Research 84(3): 312–325. https://doi.org/10.1016/j.yqres.2015.09.002

Li X-Y, Jin H-J, Wang H-W, Marchenko SS, Shan W, Luo D-L, He R-X, Spektor V, Huang Y-D, Li X-Y, Jia N (2021) Influences of forest fires on the permafrost environment: A review. Advances in Climate Change Research 12(1): 48–56. https://doi.org/10.1016/j.accre.2021.01.001

Loiko S, Raudina T, Lim A, Kuzmina D, Kulizhskiy S, Pokrovsky O (2019) Microtopography controls of carbon and related elements distribution in the west siberian frozen bogs. Geosciences 9(7): 291. https://doi.org/10.3390/geosciences9070291

Loiko S, Klimova N, Kuzmina D, Pokrovsky O (2020) Lake drainage in permafrost regions produces variable plant communities of high biomass and productivity. Plants 9(7): 867. https://doi.org/10.3390/plants9070867

Loiko SV, Kuz'mina DM, Dudko AA, Konstantinov AO, Vasil'eva YuA, Kurasova AO, Lim AG, Kulizhskii SP (2022) Charcoals in the Middle Taiga Podzols of Western Siberia as

an Indicator of Geosystem History. Eurasian Soil Science 55(2): 176–192. https://doi.org/10.1134/S1064229322020089

Loiko SV, Klimova NV, Kritckov IV, Kuzmina DM, Kulizhsky SP (2023) Soils and vegetation of the riverside floodplain in the hydrological continuum of the southern tundra within the Pur–Taz interfluve (Western Siberia). Acta Biologica Sibirica 9: 293–315. https://doi.org/10.5281/zenodo.7879848

Luo Y, Yu Z, Zhang K, Xu J, Brookes PC (2016) The properties and functions of biochars in forest ecosystems. Journal of Soils and Sediments 16(8): 2005–2020. https://doi.org/10.1007/s11368-016-1483-5

Mekonnen ZA, Riley WJ, Randerson JT, Shirley IA, Bouskill NJ, Grant RF (2022) Wildfire exacerbates high-latitude soil carbon losses from climate warming. Environmental Research Letters 17(9): 094037. https://doi.org/10.1088/1748-9326/ac8be6

Mergelov N, Zazovskaya E, Fazuldinova N, Petrov D, Dolgikh A, Matskovsky V, Golyeva A, Bichurin R, Miamin V, Dobryansky A (2024) Chronology and properties of macrocharcoal sequestered in boreal forest soils since deglaciation (southeast of the Kola Peninsula). Catena 236: 107753. https://doi.org/10.1016/j.catena.2023.107753

Mooney S, Tinner W (2011) The analysis of charcoal in peatand organic sediments. Mires and Peat 7(9): 1–18.

Moskovchenko DV, Aref'ev SP, Moskovchenko MD, Yurtaev AA (2020) Spatiotemporal Analysis of Wildfires in the Forest Tundra of Western Siberia. Contemporary Problems of Ecology 13(2): 193–203. https://doi.org/10.1134/S1995425520020092

Nelson K, Thompson D, Hopkinson C, Petrone R, Chasmer L (2021) Peatland-fire interactions: A review of wildland fire feedbacks and interactions in Canadian boreal peatlands. Science of the Total Environment 769: 145212. https://doi.org/10.1016/j.scitotenv.2021.145212

Novenko E, Rudenko O, Mazei N, Kupriyanov D, Andreev R, Shatunov A, Kusilman M, Prokushkin A, Olchev A (2023) Effects of Climate Change and Fire on the Middle and Late Holocene Forest History in Yenisei Siberia. Forests 14(12): 2321. https://doi.org/10.3390/f14122321

Novenko EYu, Kupryanov DA, Mazei NG, Prokushkin AS, Phelps LN, Buri A, Davis BAS (2022) Evidence that modern fires may be unprecedented during the last 3400 years in permafrost zone of Central Siberia, Russia. Environmental Research Letters 17: 025004. https://doi.org/10.1088/1748-9326/ac4b53

Nurrohman RK, Kato T, Ninomiya H, Végh L, Delbart N, Miyauchi T, Sato H, Shiraishi T, Hirata R (2024) Future projections of Siberian wildfire and aerosol emissions. Biogeosciences 21: 4195–4227. https://doi.org/10.5194/bg-21-4195-2024

Opokina OL, Slagoda EA, Ivanov VI, Khomutov AV, Kuznetsova AO, Danko MM, Koroleva ES, Simonova GV (2024) Formation of the trough-ridge relief of the Pur-Taz interfluve in the late Pleistocene–Holocene. Earth's Cryosphere 28(3): 3–18. https://doi.org/10.15372/KZ20240301 [In Russian]

Palmtag J, Hugelius G, Lashchinskiy N, Tamstorf MP, Richter A, Elberling B, Kuhry P (2015) Storage, Landscape Distribution, and Burial History of Soil Organic Matter in Con-

trasting Areas of Continuous Permafrost. Arctic, Antarctic, and Alpine Research 47(1): 71–88. https://doi.org/10.1657/aaar0014-027

Parham LM, Prokushkin AS, Pokrovsky OS, Titov SV, Grekova E, Shirokova LS, McDowell WH (2013) Permafrost and fire as regulators of stream chemistry in basins of the Central Siberian Plateau. Biogeochemistry 116: 55–68. https://doi.org/10.1007/s10533-013-9922-5

Pastukhov A, Marchenko-Vagapova T, Loiko S, Kaverin D (2021) Vulnerability of the Ancient Peat Plateaus in Western Siberia. Plants 10(12): 2813. https://doi.org/10.3390/plants10122813

Pellegrini AFA, Ahlström A, Hobbie SE, Reich PB, Nieradzik LP, Staver AC, Scharenbroch BC, Jumpponen A, Anderegg WRL, Randerson JT, Jackson RB (2018) Fire frequency drives decadal changes in soil carbon and nitrogen and ecosystem productivity. Nature 553(7687): 194–198. https://doi.org/10.1038/nature24668

Peteet D, Andreev A, Bardeen W, Mistretta F (1998) Long-term Arctic peatland dynamics, vegetation and climate history of the Pur-Taz region, Western Siberia. Boreas 27: 115–126. https://doi.org/10.1111/j.1502-3885.1998.tb00872.x

Pupysheva MA, Blyakharchuk TA (2024) Reconstruction of the Holocene paleo-fire history in the middle taiga subzone of Western Siberia according to the macro-charcoal analysis of lake sediments. Geosphere Research 1: 135–151. https://doi.org/10.17223/25421379/30/8 [In Russian]

Pupysheva MA, Blyakharchuk TA (2023) Fires and their Significance in the Earth's Post-Glacial Period: a Review of Methods, Achievements, Groundwork. Contemporary Problems of Ecology 16(3): 303–315. https://doi.org/10.1134/S1995425523030095

Reimer PJ, Austin WEN, Bard E, Bayliss A, Blackwell PG, Bronk Ramsey C, Butzin M, Cheng H, Edwards RL, Friedrich M, Grootes PM, Guilderson TP, Hajdas I, Heaton TJ, Hogg AG, Hughen KA, Kromer B, Manning SW, Muscheler R, Palmer JG, Pearson C, van der Plicht J, Reimer RW, Richards DA, Scott EM, Southon JR, Turney CSM, Wacker L, Adolphi F, Büntgen U, Capano M, Fahrni SM, Fogtmann-Schulz A, Friedrich R, Köhler P, Kudsk S, Miyake F, Olsen J, Reinig F, Sakamoto M, Sookdeo A, Talamo S (2020) The IntCal20 Northern Hemisphere Radiocarbon Age Calibration Curve (0–55 calkBP). Radiocarbon 62(4): 725–757. https://doi.org/10.1017/RDC.2020.41

Ryabogina NE, Nesterova MI, Utaygulova RR, Trubitsyna ED (2024) Forest fires in south-west Western Siberia: the impact of climate and economic transitions over 9000 years. Journal of Quaternary Science 39(3): 432–442. https://doi.org/10.1002/jqs.3593

Scholten RC, Veraverbeke S, Chen Y, Randerson JT (2024) Spatial variability in Arctic–boreal fire regimes influenced by environmental and human factors. Nature Geoscience 17(9): 866–873. https://doi.org/10.1038/s41561-024-01505-2

Shefer NV, Blyakharchuk TA, Loiko SV, Shumilovskikh LS, Gureyeva II (2023) History of vegetation and fires in the Arctic part of the Pur-Taz interfluve in the Holocene. Arctic and Antarctic Research 69(2): 244–263. https://doi.org/10.30758/0555-2648-2023-69-2-244-263 [In Russian]

Shestakova TA, Rogers BM, Mackey B, Hugh S, Norman P, Kukavskaya EA (2024) Tracking ecosystem stability across boreal Siberia. Ecological Indicators 169: 112841. https://doi.org/10.1016/j.ecolind.2024.112841

Shumilovskikh LS, Shumilovskikh ES, Schlütz F, van Geel B (2022) NPP-ID – Non-Pollen Palynomorphs Image Database as a research and educational platform. Vegetation History and Archaeobotany 31: 323–328. https://doi.org/10.1007/s00334-021-00849-8

Shumilovskikh LS, Shumilovskikh ES, Schlütz F, van Geel B (2022) Correction: NPP-ID – Non-Pollen Palynomorphs Image Database as a research and educational platform. Vegetation History and Archaeobotany 31: 323–328. https://doi.org/10.1007/s00334-021-00849-8

Sizov O, Ezhova E, Tsymbarovich P, Soromotin A, Prihod'ko N, Petäjä T, Zilitinkevich S, Kulmala M, Bäck J, Köster K (2021) Fire and vegetation dynamics in northwest Siberia during the last 60 years based on high-resolution remote sensing. Biogeosciences 18: 207–228. https://doi.org/10.5194/bg-18-207-2021

Startsev V, Gorbach N, Mazur A, Prokushkin A, Karpenko L, Dymov A (2022) Macrocharcoal Signals in Histosols Reveal Wildfire History of Vast Western Siberian Forest-Peatland Complexes. Plants 11(24): 3478. https://doi.org/10.3390/plants11243478

Stepanova OB, Syuzyumov AA (2019) The Taz and Turukhan basins on geographical maps of the 18th-first half of the 20th centuries. Bulletin of Bryansk State University 3(41): 59–71. [In Russian]

Stivrins N, Aakala T, Pasanen L, Kuuluvainen T, Vasanda H, Gałka M, Disbrey HR, Liepins J, Holmström L, Seppä H (2019) Integrating fire-scar, charcoal and fungal spore data to study fire events in the boreal forest of northern Europe. The Holocene 29(9): 1480–1490. https://doi.org/10.1177/0959683619854524

Stockmarr JA (1971) Tabletes with spores used in absolute pollen analysis. Pollen spores 13: 615–621.

Talucci AC, Loranty MM, Alexander HD (2022) Siberian taiga and tundra fire regimes from 2001–2020. Environmental Research Letters 17(2): 025001. https://doi.org/10.1088/1748-9326/ac3f07

Tikhonravova Y, Kuznetsova A, Slagoda E, Koroleva E (2023) Holocene permafrost peatland evolution in drained lake basins on the Pur-Taz Interfluve, North-Western Siberia. Quaternary International 669: 32–42. https://doi.org/10.1016/j.quaint.2023.07.005

Tkachev AA, Tkachev AA (2019) On the history of the development of the Tazovsky Arctic in ancient times. In: Tyumen region: historical retrospective, realities of the present, contours of the future. Collection of articles from the international conference, Tyumen-Tobolsk, September 2019. Industrial University of Tyumen Publishers, Tyumen, 344–351. [In Russian]

Tkachev AA (2018) Research on the territory of the Tazovsky district of the Yamalo-Nenets Autonomous Okrug. Archaeological discoveries 2016: 364–366. https://doi.org/10.25681/IARAS.2018.978-5-94375-260-5.364-366 [In Russian]

Turunen J, Tahvanainen T, Tolonen K, Pitkänen A (2001) Carbon accumulation in West Siberian mires, Russia. Global Biogeochemical Cycles 15(2): 285–296. https://doi.org/10.1029/2000GB001312

Vachula RS, Sae-Lim J, Russell JM (2020) Sedimentary charcoal proxy records of fire in Alaskan tundra ecosystems. Palaeogeography, Palaeoclimatology, Palaeoecology 541: 109564. https://doi.org/10.1016/j.palaeo.2019.109564

Van Geel B, Gelorini V, Lyaruu A, Aptroot A, Rucina S, Marchant R, Sinninghe JS, Damsté D, Verschuren D (2011) Diversity and ecology of tropical African fungal spores from a 25,000-year palaeoenvironmental record in southeastern Kenya. Review of Palaeobotany and Palynology 164(3–4): 174–190. https://doi.org/10.1016/j.revpalbo.2011.01.002

Vasil'chuk YK, Vasil'chuk AC (2016) Thick polygonal peatlands in continuous permafrost zone of West Siberia. Earth's Cryosphere 20(4): 3–13.

Whitlock C, Larsen C (2001) Charcoal as a fire proxy. In: Smol, JP, Birks HJB, Last WM (Eds) Tracking Environmental Change using Lake Sediments. Volume 3: Terrestrial, Algal, and Siliceous Indicators. Springer Book Archive, 76–92.

Zarov EA, Golubyatnikov LL, Lapshina ED, Loyko SV (2021) Vegetation and soils of tundra landscapes in the Pur-Taz interfluvial region. Biology Bulletin 48: 118–127. https://doi.org/10.1134/S1062359022010186

Zhao W, Li H, Chen C, Renssen H (2022) Large-scale vegetation response to the 8.2 ka BP cooling event in East Asia. Palaeogeography, Palaeoclimatology, Palaeoecology 608: 111303. https://doi.org/10.1016/j.palaeo.2022.111303